Infrared, Resonance Raman, and Excitation Profile Studies of $Os_2(O_2CCH_3)_4Cl_2$ and $Os_2(O_2CCD_3)_4Cl_2$. The Assignment of the Osmium–Osmium Stretching Vibration for a Complex Involving an Osmium–Osmium Multiple Bond

Robin J. H. Clark,* Andrew J. Hempleman, and Derek A. Tocher

Contribution from the Christopher Ingold Laboratories, University College London, 20 Gordon Street, London WC1H 0AJ, U.K. *Received January 25, 1988*

Abstract: Extensive Raman studies (1525–40 cm^{-1}) of $Os_2(O_2CCH_3)_4Cl_2$ have led to the identification of the three strong bands, ν_1, ν_2, and ν_3, at 229, 393, and 292 cm^{-1} to the key skeletal stretching modes, ν(OsOs), ν(OsO), and ν(OsCl), respectively. Raman spectra of the complex at resonance with the intense electronic band at λ_{max} = 383 nm lead to the development of a six-membered overtone progression in ν_1 as well as combination band progressions in ν_1 based upon one quantum of either ν_2 or ν_3. This indicates that the principal structural change attendant upon excitation to the resonant state is along the OsOs coordinate. Fourier transform infrared spectra (3500–40 cm^{-1}) have also been obtained. Acetate deuteriation provides conclusive evidence for many of the infrared and Raman band assignments. The study provides the first firm identification of ν(OsOs) for a multiply bonded species.

Following the X-ray determination of the structure of $Re_2(O_2CC_6H_5)_4Cl_2$ in 1968[1] the chemistry of third-row dimetal tetracarboxylates began to be developed. However, there were no reports on possible diosmium complexes until that by Wilkinson et al.[2] regarding a brown osmium(III) chloroacetate of stoicheiometry $[Os(O_2CCH_3)_2Cl]_n$. Shortly afterwards the X-ray crystal structure of the analogous butyrate complex was determined[3,4] and shown to possess the familiar dimeric tetracarboxylate framework

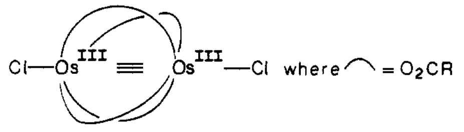

Since this time the crystal structures of $Os_2(O_2CCH_3)_4Cl_2$ and $Os_2(O_2CC_2H_5)_4Cl_2$ have also been determined,[5] the tetracarboxylate framework being virtually identical for all three complexes. The average OsOs distance in these complexes is 2.310 Å, consistent with the formal OsOs triple bond that should result from their d^5–d^5 configuration. All such complexes are air stable and, surprisingly, paramagnetic, with μ = 2.0–1.6 μ_B at room temperature; this implies either[3] that there is an equilibrium between the two possible ground-state configurations, δ^{*2} and $\delta^*\pi^*$ or, more probably, that the moment represents the expected value for the ^3E_u (δ^* π^*) term split by first-order spin-orbit coupling.[6]

As an extension of earlier vibrational studies of dirhodium[7-9] and diruthenium tetracarboxylates,[10] we have embarked on a systematic vibrational study of the diosmium analogues with the view, in particular, of assigning the key skeletal modes ν(OsOs), ν(OsO), and ν(OsCl). This is difficult, since all three types of mode are expected to occur in the 400–200-cm^{-1} region. Moreover, although there may be little coupling between ν(OsOs) and ν(OsO), owing to the fact that the angles OsOsO are near 90°, significant coupling between the coaxial modes ν(OsOs) and ν(OsCl) may be expected. Thus in order to place the band assignments on a firm basis it is essential to study both $Os_2(O_2CCH_3)_4Cl_2$ as well as $Os_2(O_2CCD_3)_4Cl_2$. This has now been accomplished, and the results are reported herein.

Experimental Section

Preparations of Complexes. The complex $Os_2(O_2CCH_3)_4Cl_2$ was prepared by the established procedure.[3] The deuteriate was prepared from $[Ph_4N]_2[Os_2Cl_8]$[11,12] by use of acetic acid 100.0 atom% D and acetic anhydride 99+ atom% D (Aldrich). Elemental analyses for C, H, and Cl were satisfactory. Attempts to isolate an analogous bromide for comparative studies were not successful, unsatisfactory analyses being invariably obtained.

Instrumental. Raman spectra were recorded by use of a Spex 14018 (R6) spectrometer in conjunction with Coherent CR 3000 K and CR 12 lasers. Samples were held as pressed KCl discs at ca. 80 K in a liquid nitrogen cell.

Infrared spectra were recorded at ca. 80 K as KCl discs (3500–500 cm^{-1}) and as pressed wax discs (660–40 cm^{-1}) at a spectral resolution of 1 cm^{-1} with a Bruker 113 V interferometer (for details of disc preparations see ref 8). Overlap between mid- and far-infrared regions allowed matching of band intensities, which are quoted on an arbitrary intensity scale of vw < 0.02, w 0.02–0.2, m 0.2–0.6, s 0.6–0.9, vs > 0.9; br = broad, sh = shoulder.

The 20 K solid-state transmission spectrum (700–230 nm) of $Os_2(O_2CCH_3)_4Cl_2$ was obtained, as a pressed disc of the complex dispersed in KCl, by use of a Cary 14 spectrometer in conjunction with an Air Products Displex system: band maxima/nm, 246 s, 274 s, and 383 s.

Results and Discussion

Raman Spectra. Unlike dirhodium tetracarboxylates for which Raman spectra are obtainable with any available excitation line, diosmium tetracarboxylates yield only poor Raman spectra unless recorded at or near resonance with a fully allowed transition. The electronic spectrum of $Os_2(O_2CCH_3)_4Cl_2$ as a KCl disc at ca. 20 K is characterized by an intense band at λ_{max} = 383 nm. Excitation within the contour of this band, viz. with λ_0 = 406.7 nm (Figure 1), yields a resonance Raman spectrum which is dominated by a very intense band at 229 cm^{-1} denoted ν_1, by an associated overtone progression (reaching $6\nu_1$), and by two combination band progressions (reaching $3\nu_1 + \nu_2$ and $4\nu_1 + \nu_3$, where ν_2 and ν_3 are Raman-active fundamentals at 393 and 292 cm^{-1}, respectively). Detailed band listings both for the proteo as well

---

(1) Bennett, M. J.; Bratton, W. K.; Cotton, F. A.; Robinson, W. R.; *Inorg. Chem.* **1968**, *7*, 1570–1575.

(2) Moore, D. S.; Alves, A. S.; Wilkinson, G. *J. Chem. Soc., Chem. Commun.* **1981**, 1164–1165.

(3) Behling, T.; Wilkinson, G.; Stephenson, T. A.; Tocher, D. A.; Walkinshaw, M. D. *J. Chem. Soc., Dalton Trans.* **1983**, 2109–2116.

(4) Stephenson, T. A.; Tocher, D. A.; Walkinshaw, M. D. *J. Organomet. Chem.* **1982**, *232*, C51–C54.

(5) Cotton, F. A.; Chakravarty, A. R.; Tocher, D. A.; Stephenson, T. A. *Inorg. Chim. Acta* **1984**, *87*, 115–119.

(6) Miskowski, V. M.; Gray, H. B., to be published.

(7) Clark, R. J. H.; Hempleman, A. J.; Flint, C. D. *J. Am. Chem. Soc.* **1986**, *108*, 518–520.

(8) Clark, R. J. H.; Hempleman, A. J. *Inorg. Chem.*, in press.

(9) Clark, R. J. H.; Hempleman, A. J. *Croat. Chim. Acta*, in press.

(10) Clark, R. J. H.; Ferris, L. T. H. *Inorg. Chem.* **1981**, *20*, 2759–2766.

(11) Fanwick, P. E.; King, M. K.; Tetrick, S. M.; Walton, R. A. *J. Am. Chem. Soc.* **1985**, *107*, 5009–5011.

(12) Agaskar, P. A.; Cotton, F. A.; Dunbar, K. R.; Falvello, L. R.; Tetrick, S. M.; Walton, R. A. *J. Am. Chem. Soc.* **1986**, *108*, 4850–4855.

0002-7863/88/1510-5968$01.50/0 © 1988 American Chemical Society

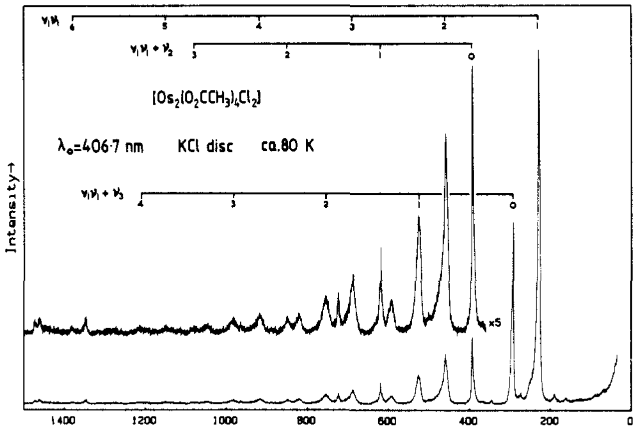

Figure 1. Resonance Raman spectrum (1525–40 cm^{-1}) of $Os_2(O_2CCH_3)_4Cl_2$ as a KCl disc at ca. 80 K with 406.7-nm excitation. Resolution ca. 2 cm^{-1}.

Table I. Wavenumbers (cm^{-1}) of Bands Observed in the Resonance Raman Spectrum[a] of [$Os_2(O_2CCH_3)_4Cl_2$] at ca. 80 K

$\tilde{\nu}$	assignment	$\tilde{\nu}$	assignment
161 vw		688 w, br	$3\nu_1$
190 vw		702 vw, br	$2\nu_1 + 249$
229 vs	ν_1, ν(Os–Os)	723 vw	δ(OCO)
237 m, sh		754 vw, br	$2\nu_1 + \nu_3$
249 w, sh		776 vw, sh	
273 vw		820 vw, br	$\nu_1 + 2\nu_3$
292 s	ν_3, ν(Os–Cl)	826 vw, sh	
296 m, sh	ν(Os–Cl)	849 vw, br	$2\nu_1 + \nu_2$
305 vw, sh	ν(Os–Cl)	917 vw, br	$4\nu_1$
346 vw	ν(Os–O)	965 vw	ν(C–C)
386 w, sh	ν(Os–O)	982 vw, br	$3\nu_1 + \nu_3$
390 w, sh	ν(Os–O)	1048 vw, br	$\rho(CH_3)$
393 m	ν_2, ν(Os–O)	1079 vw, br	$3\nu_1 + \nu_2$
458 w	$2\nu_1$	1115 vw	$\nu_2 + \delta$(OCO)
468 w, sh	$\nu_1 + 237$	1148 vw, br	$5\nu_1$
479 w, sh	$\nu_1 + 249$	1214 vw, br	$4\nu_1 + \nu_3$
525 w, br	$\nu_1 + \nu_3$	1348 vw	$\delta_s(CH_3)$
592 vw, br	$2\nu_3$	1379 vw	$6\nu_1$
619 w	$\nu_1 + \nu_2$	1460 vw	$\delta_{as}(CH_3)$
631 vw	ρ_w(COO)	1472 vw	ν_{as}(COO)

[a] = 406.7-nm excitation.

Table II. Wavenumbers (cm^{-1}) of Bands Observed in the Resonance Raman Spectrum[a] of [$Os_2(O_2CCD_3)_4Cl_2$] at ca. 80 K

$\tilde{\nu}$	assignment	$\tilde{\nu}$	assignment
183 vw		592 vw	ρ_r(COO)/$2\nu_3$
223 m, sh		602 vw	$\nu_1 + \nu_2$
230 vs	ν_1, ν(Os–Os)	651 vw	
249 w, sh		672 vw	$\nu_2 + \nu_3$
272 vw		684 vw	
280 vw		690 vw	$3\nu_1$
293 s	ν_3, ν(Os–Cl)	699 vw	δ(OCO)
296 m, sh	ν(Os–Cl)	747 vw, sh	$2\nu_2$
302 w, sh	ν(Os–Cl)	755 vw	$2\nu_1 + \nu_3$
327 vw	ν(Os–O)	827 vw	
353 vw, br		899 vw	$\nu_1 + \nu_2 + \nu_3$
367 vw		913 vw	ν(C–C)/$4\nu_1$(?)
370 w, sh	ν(Os–O)	981 vw, br	$3\nu_1 + \nu_3$
374 w, sh	ν(Os–O)	1053 vw, br	
375 m	ν_2, ν(Os–O)	1100 vw	$\delta_s(CD_3)$
459 w	$2\nu_1$	1140 vw, br	
471 w, sh		1210 vw, br	$4\nu_1 + \nu_3$
478 w, sh	$\nu_1 + 249$	1410 vw	ν_s(COO)
527 w, br	$\nu_1 + \nu_3$	1467 vw	ν_{as}(COO)
577 vw			

[a] = 406.7-nm excitation.

as for the deuterio forms (vide infra) are given in Tables I and II, respectively. No Raman spectra were detected at resonance with the weak transitions (e.g., $\delta \rightarrow \delta^*$ at 850 nm)[6] originating from the $^3E_u(\delta^*\pi^*)$ ground state.

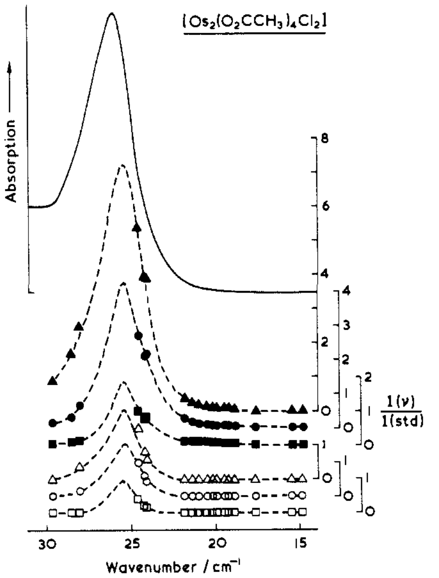

Figure 2. Excitation profiles of ν_1 (▲), ν_2 (■), ν_3 (●), $2\nu_1$ (△), $\nu_1 + \nu_2$ (□), and $\nu_1 + \nu_3$ (○) for $Os_2(O_2CCH_3)_4Cl_2$ at ca. 80 K together with the transmission electronic spectrum as a KCl disc at ca. 20 K.

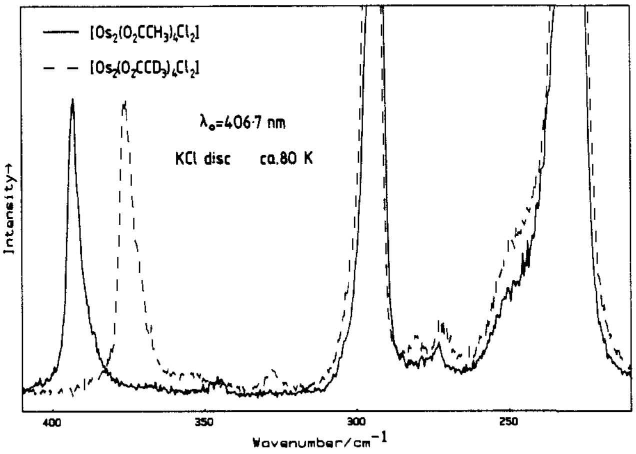

Figure 3. Resonance Raman spectra (410–210 cm^{-1}) of $Os_2(O_2CCH_3)_4Cl_2$ (—) and $Os_2(O_2CCD_3)_4Cl_2$ (– –) (ν_1 and ν_3 bands truncated) as KCl discs at ca. 80 K with 406.7-nm excitation. Resolution ca. 2 cm^{-1}.

Excitation profiles (EP's) have been constructed for the bands attributed to ν_1, ν_2, ν_3, $2\nu_1$, $\nu_1 + \nu_2$, and $\nu_1 + \nu_3$ (Figure 2). These demonstrate that all of the Raman bands reach their maximum intensities within the contour of the 383-nm electronic band, although the exact wavenumber of the EP maxima could not be determined owing to the lack of suitable exciting lines at all desired wavenumbers. Clearly, ν_1, ν_2, and ν_3 are all strongly coupled to the 383-nm band, which appears with axial polarization and is assigned to the $\pi(Cl) \rightarrow \pi^*(Os_2)$ transition;[6] moreover, all three modes are likely to be totally symmetric, owing to their involvement in resonance Raman progressions.

The assignment of the three bands in the 400–200 cm^{-1} region is difficult owing to the expectation that all three key skeletal stretching fundamentals, viz. ν(OsOs), ν(OsO), and ν(OsCl), could have similar wavenumbers—at least to within a factor of two. Thus it was considered essential to synthesize and study the perdeuterio analogue since this has provided a means for the unambiguous identification of ν(MoO) for $Mo_2(O_2CCH_3)_4$.[13]

Assignments of Raman-Active Fundamentals. **ν(OsOs).** The band at 229 cm^{-1}, denoted ν_1, is assigned to ν(OsOs) on the grounds that (a) it is the most likely candidate on the basis of mass considerations; (b) it forms the dominant progression-forming

---

(13) Hempleman, A. J.; Clark, R. J. H.; Flint, C. D. *Inorg. Chem.* **1986**, *25*, 2915–2916. Clark, R. J. H.; Hempleman, A. J.; Kurmoo, M.; *J. Chem. Soc., Dalton Trans.* **1988**, 973–981.

Table III. Vibrational Structural Data for Related Dinuclear Cage Structures

complex	ν(MM) (cm^{-1})	r(MM) (Å)	ν(MCl) (cm^{-1})	r(MCl) (Å)
$[Pt_2(P_2O_5H_2)_4Cl_2]^{4-}$	158^a	2.695^b	305^a	2.407^b
$Os_2(O_2CCH_3)_4Cl_2$	229^c	2.314^d	292^c	2.448^d
$Re_2(O_2CC_6H_5)_4Cl_2$	295^e	2.235^f	248^e	2.489^f
$Ru_2(O_2CCH_3)_4Cl$	326^g	2.287^{h,i}	159^g	2.577^{h,i}

[a] Kurmoo, M.; Clark, R. J. H. *Inorg. Chem.* **1985**, *24*, 4420–4425. [b] Chê, C.-M.; Herbstein, F. H.; Schaefer, W. P.; Marsh, R. E.; Gray, H. B. *J. Am. Chem. Soc.* **1983**, *105*, 4604–4607. [c] This work. [d] Reference 5. [e] Oldham, C.; Davies, J. E. D.; Ketteringham, A. P. *J. Chem. Soc., Chem. Commun.* **1971**, 572–573. [f] Reference 1. [g] Reference 22. [h] Reference 16. [i] A more obvious ruthenium analogue would be $[Ru_2(O_2CCH_3)_4Cl_2]^-$; however, although structural data exist for this ion (reference 16, r(MM) = 2.286 Å, r(MCl) = 2.521 Å), no Raman data are yet available.

mode, this feature being a characteristic of the Raman spectra of metal–metal multiply bonded species taken at resonance with electronic transitions involving substantial change of metal character;[14,15] and (c) it suffers no shift (to within 1 cm^{-1}) on deuteriation, as expected for a mode which is virtually orthogonal to the ν(OsO) modes (Figure 3).

From the wavenumbers of the bands in the $v_1\nu_1$ progression (v_1 = vibrational quantum number), it is evident that ν_1 is almost exactly harmonic, the anharmonicity constant, x_{11}, being 0.0 ± 0.1 cm^{-1}.

Although $Os_2(O_2CCH_3)_4Cl_2$ is insufficiently soluble for measurements of depolarization ratios, both $Os_2(O_2CC_2H_5)_4Cl_2$ and $Os_2(O_2CC_3H_7)_4Cl_2$ are. At resonance the ρ values (0.38 and 0.37, respectively) imply not only that ν_1 is polarized and therefore totally symmetric but that the resonant electronic transition must be axially polarized.

ν(OsO). The band at 393 cm^{-1}, denoted ν_2, is assigned to ν(OsO) on the basis that it and it alone (of ν_1, ν_2, and ν_3) is shifted to lower wavenumber by a substantial amount (18 cm^{-1}) on deuteriation. The ratio of the ν_2 values for the deuterio and proteo forms (0.95) is comparable with that found for the analogous modes of $Mo_2(O_2CCH_3)_4$ (0.97)[13] and $Rh_2(O_2CCH_3)_4(PPh_3)_2$ (0.96).[8] Although one might not expect there to be a very close correlation between ν(MO) and r(MO) for dimetal tetracarboxylates, nevertheless a moderate correlation is apparent: thus, for the series $Os_2(O_2CCH_3)_4Cl_2$, $Ru_2(O_2CCH_3)_4Cl$, $Rh_2(O_2CCH_3)_4(PPh_3)_2$, and $Mo_2(O_2CCH_3)_4$, ν(MO) decreases in the order 393, 372,[10] 338,[8] and 323[13] cm^{-1}, respectively, in parallel with the increase in r(MO) in the order 2.009,[5] 2.018,[16] 2.045,[17] and 2.119 Å,[18] respectively.

ν(OsCl). The third intense band (at 292 cm^{-1}) in the 400–200 cm^{-1} region, denoted ν_3, is assigned to ν(OsCl) on the grounds that (a) this band occurs at a wavenumber similar to that found for ν(OsCl) for other octahedrally coordinated osmium complexes containing OsCl bonds, viz. $Os(CO)_4Cl_2$ (298, 328 cm^{-1})[19] and $Os(CO)_4(HgCl)Cl$ (320 cm^{-1})[20] and (b) it is unshifted (to within 1 cm^{-1}) on deuteriation of the complex, as expected for a mode which should be virtually uncoupled from ν(CH) modes and as distinct from ν(OsO) modes.

Considerable coupling between OsOs and OsCl symmetry coordinates is expected since the latter are coaxial and share a common atom—a situation[21] which is found for many other structurally related complexes (Table III). Thus $Os_2(O_2CCH_3)_4Cl_2$ is similar to the diphosphite ion $[Pt_2(P_2O_5H_2)_4Cl_2]^{4-}$ in that $\nu(MM) < \nu(MCl)$, where M = metal; the coupling of these coordinates has the effect of lowering ν(MM) but raising ν(MCl) from their expected wavenumbers as uncoupled oscillators. The converse is true for $Re_2(O_2CC_6H_5)_4Cl_2$ and $Ru_2(O_2CCH_3)_4Cl$ (the latter contains linear chlorine bridges)[16,22] for which $\nu(MM) > \nu(MCl)$; coupling of these coordinates in this case has the opposite effect, viz. it leads to a raising of ν(MM) and a lowering of ν(MCl) from their expected wavenumbers as uncoupled oscillators. The expected reciprocal relationship between ν(MCl) and r(MCl) is apparent from the data listed in Table III; the relationship is less clear cut for ν(MM) and r(MM), owing to the complication that much of the metal–metal restoring force has, as its basis, not the intrinsic metal–metal bond order and thus force constant but the four OCO bending force constants. It is also obvious from Table III that there is a reciprocal relationship between ν(MM) and ν(MCl).

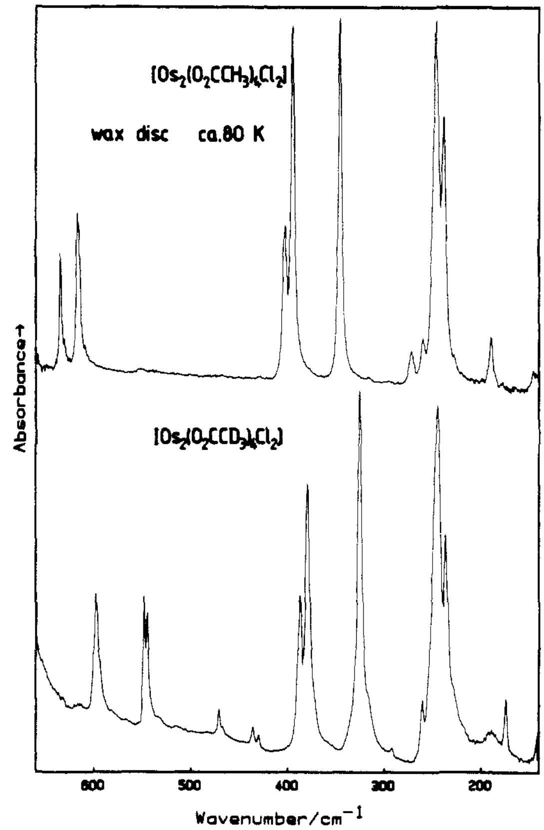

Figure 4. FTIR spectra (660–140 cm^{-1}) of $Os_2(O_2CCH_3)_4Cl_2$ and $Os_2(O_2CCD_3)_4Cl_2$ as wax discs at ca. 80 K.

The two main bands attributed to ν_2 and ν_3 show evidence of structure and/or shoulders which may be related to site and/or correlation effects (there are two molecules per unit cell).[5] Shoulders on the low wavenumber side of ν_2 are assigned (Table I) to other (non-a_{1g}) ν(OsO) fundamentals on the basis of their similar shifts to ν_2 on deuteriation.

Other Modes. Other band assignments are included in Tables I and II.

Infrared Spectra ν(OsO). The infrared spectra (660–140 cm^{-1}) of $Os_2(O_2CCH_3)_4Cl_2$ and $Os_2(O_2CCD_3)_4Cl_2$ as wax discs at ca. 80 K are shown in Figure 4. Bands for the former at 403, 395, and 346 cm^{-1} which shift on deuteriation to 387, 379, and 326 cm^{-1} (average shift 17 cm^{-1}) are assigned to ν(OsO), cf. the near identical shift of the Raman-active ν(OsO) fundamentals (18 cm^{-1}, vide supra) on deuteriation. Only two such fundamentals (a_{2u} + e_u) should be infrared active if the molecule could truly be approximated to a $M_2(O_2CR)_4L_2$ species of D_{4h} symmetry.[13] The

---

[14] Clark, R. J. H.; Stead, M. J. *Inorganic Chemistry: Towards the 21st Century*; Chisholm, M. H., ed.; ACS Symposium Series 211; American Chemical Society: Washington, DC, 1983; pp 235–240.

[15] Clark, R. J. H.; Stead, M. J. *Inorg. Chem.* **1983**, *22*, 1214–1220.

[16] Bino, A.; Cotton, F. A.; Felthouse, T. R. *Inorg. Chem.* **1979**, *18*, 2599–2604.

[17] Christoph, G. G.; Halpern, J.; Khare, G. P.; Koh, Y. B.; Romanowski, C. *Inorg. Chem.* **1981**, *20*, 3029–3037.

[18] Cotton, F. A.; Mester, Z. C.; Webb, T. R. *Acta Crystallogr., Sect. B: Struct. Crystallogr. Cryst. Chem.* **1974**, *30*, 2768–2770.

[19] Bennett, M. A.; Clark, R. J. H. *J. Chem. Soc.* **1964**, 5560–5568.

[20] Bradford, C. W.; van Bronswyk, W.; Clark, R. J. H.; Nyholm, R. S. *J. Chem. Soc. A* **1968**, 2456–2463.

[21] Stein, P.; Dickson, M. K.; Roundhill, D. M. *J. Am. Chem. Soc.* **1983**, *105*, 3489–3494.

[22] Miskowski, V. M.; Loehr, T. M.; Gray, H. B. *Inorg. Chem.* **1987**, *26*, 1098–1108.

Figure 5. FTIR spectra (1600–600 cm^{-1}) of $Os_2(O_2CCH_3)_4Cl_2$ and $Os_2(O_2CCD_3)_4Cl_2$ as KCl discs at ca. 80 K.

observation of three bands implies that the four R groups have lowered the symmetry of the molecule with the consequence that the degeneracy of the e_u mode has been resolved, presumably into the 403 and 395 cm^{-1} bands in the proteo form and into the 387 and 379 cm^{-1} bands in the deuterio form.

ν(OsCl). The bands at 247 (with shoulders at 248 and 245 cm^{-1}) and 239 cm^{-1} in the infrared spectrum of $Os_2(O_2CCH_3)_4Cl_2$ are assigned to ν(OsCl). They have weak Raman counterparts and are virtually unshifted on deuteriation. Only one asymmetric OsCl stretching mode should be infrared active (a_{2u} species) for the isolated molecule, and hence the appearance of more than this implies the presence of site and/or factor group effects (possibly complicated by chlorine isotopic effects). As is not unusual for vibrations of heavy metal complexes, ν_{asym}(OsCl), ~243 cm^{-1} < ν_{sym}(OsCl), 292 cm^{-1}, cf. the same situation for the complexes $[Pt_2(P_2O_5H_2)_4X_2]^{4-}$, X = Cl, Br, or I.[21] However for $Re_2(O_2CCH_3)_4Cl_2$ the infrared- and Raman-active ν(ReCl) fundamentals are virtually coincident, while for the much lighter and chain polymeric complex $Ru_2(O_2CCH_3)_4Cl$ the situation is reversed, with ν_{asym}(RuCl) being 40 cm^{-1} above ν_{sym}(RuCl).[22]

Other Modes. The infrared spectra of $Os_2(O_2CCH_3)_4Cl_2$ and $Os_2(O_2CCD_3)_4Cl_2$ in the region 1600–600 cm^{-1} (Figure 5) are in general similar to those of related complexes such as $Mo_2(O_2CCH_3)_4$ and $Mo_2(O_2CCD_3)_4$.[13] The OCO bend is clearly observed as a doublet at 700 and 695 cm^{-1}, shifting to 682, 679, and 674 cm^{-1} on deuteriation. The Raman counterparts are at 723 and 699 cm^{-1} for $Os_2(O_2CCH_3)_4Cl_2$ and $Os_2(O_2CCD_3)_4Cl_2$, respectively.

Whereas the out-of-plane COO rock, ρ_w, is found at similar wavenumber (635 and 630 cm^{-1}) to that for $Mo_2(O_2CCH_3)_4$ (636 and 628 cm^{-1}),[13] the in-plane rock, ρ_r (618 and 616 cm^{-1}) is much higher than that found for $Mo_2(O_2CCH_3)_4$ (583 and 575 cm^{-1}).[13] This is attributed to increased coupling between ν(OsO) and ρ_r(COO) as a result of the ca. 30-cm^{-1} increase in ν(OsO) compared to ν(MoO). Upon deuteriation ρ_w(COO) shifts by ca. 85 cm^{-1} to 549 and 546 cm^{-1} and lies below ρ_r(COO) which shifts by ca. 20 cm^{-1} to 598 and 593 cm^{-1}. The much larger shift of ρ_w(COO) compared to ρ_r(COO) is consistent with the shifts observed for the analogous bands for both $Mo_2(O_2CCD_3)_4$[13] and $Na[O_2CCD_3]$.[23]

Table IV. Wavenumbers (cm^{-1}) of Bands Observed in the Infrared Spectrum of $[Os_2(O_2CCH_3)_4Cl_2]$ at ca. 80 K

$\tilde{\nu}$	assignment	$\tilde{\nu}$	assignment
3026 vw	ν(C–H)	1014 w, sh	618 + 395
2989 w		952 w, sh	ν(C–C)
2938 w, sh		950 w	
2932 w		700 s	δ(OCO)
2406 vw, br		695 s	
2392 vw, br		635 w	out-of-plane ρ_w(COO)
1708 vw, br		630 vw	
1674 vw, br	1043 + 630	618 w	in-plane ρ_r(COO)
1657 vw, br	1026 + 630	616 w	
1648 vw, br	1029 + 618	403 w	ν(Os–O)
1476 m	ν_{as}(COO)	395 m	
1456 vs, sh	$\delta_{as}(CH_3)$	346 m	
1451 vs		272 vw	
1423 m		261 vw	
1418 m, sh	ν_s(COO)	248 m, sh	ν(Os–Cl)
1393 m, sh	$\delta_{as}(CH_3)$	247 m	
1382 vs		245 m, sh	
1359 m	$\delta_s(CH_3)$	239 m	
1349 m		228 vw	
1345 m		190 w	δ(O-Os-O) or δ(Os-Os-O)
1048 m, sh	$\rho(CH_3)$	146 vw	
1045 m		129 vw	
1043 m, sh		104 vw	
1029 m			
1026 m, sh			

Table V. Wavenumbers (cm^{-1}) of Bands Observed in the Infrared Spectrum of $[Os_2(O_2CCD_3)_4Cl_2]$ at ca. 80 K

$\tilde{\nu}$	assignment	$\tilde{\nu}$	assignment
2424 w		911 m	$\rho(CD_3)$
2241 vw	ν(C–D)	908 m	
2234 vw		899 w	ν(C–C)
2200 vw		852 w	$\rho(CD_3)$
2195 vw		682 m, sh	δ(OCO)
2120 vw		679 m	
2109 vw		674 m	
1468 m, sh	ν_{as}(COO)	598 w	in-plane ρ_r(COO)
1463 s		593 vw	
1459 m, sh	911 + 549	549 w	out-of-plane ρ_w(COO)
1454 m	908 + 546	546 w	
1445 m, sh	852 + 593	470 vw	
1438 m, sh		467 vw	
1433 m, sh		435 vw	
1426 s		429 vw	
1410 vs	ν_s(COO)	387 w	ν(Os–O)
1381 w		379 w	
1375 w, sh		326 m	
1361 vw	682 + 679	317 w, sh	
1320 vw		292 vw	
1319 vw		260 vw	
1311 vw		245 m	ν(Os–Cl)
1304 vw		237 w	
1095 w	$\delta_s(CD_3)$	190 vw, br	
1088 w		174 vw	
1074 w, sh		141 vw	
1068 w		133 vw	
1033 w	$\delta_{as}(CD_3)$	125 vw	
1024 w		120 vw	
1018 w		101 vw	

There are no strong infrared bands above 1480 cm^{-1} and thus ν_{as}(COO) and ν_s(COO) must lie below this wavenumber; the medium bands at 1476 and 1418 cm^{-1}, respectively, are so assigned, these shifting to 1468 and 1410 cm^{-1}, respectively, on deuteriation. The low value for ν_{as}(COO) for this complex, cf. $Cu_2(O_2CCH_3)_4(H_2O)_2$ 1605 cm^{-1},[24] $Rh_2(O_2CCH_3)_4(PPh_3)_2$ 1595 cm^{-1},[8] $Mo_2(O_2CCH_3)_4$ 1500 cm^{-1},[13] and $Os_2(O_2CCH_3)_4Cl_2$ 1476 cm^{-1}, is consistent with the relatively long carbon–oxygen distance,

---

(23) Ito, K.; Bernstein, H. J. *Can. J. Chem.* **1956**, *34*, 170–178.

(24) Mathey, Y.; Greig, D. R.; Shriver, D. F. *Inorg. Chem.* **1982**, *21*, 3409–3413.

which is 1.260,[25] 1.260,[17] 1.277,[18] and 1.283 Å,[5] respectively, for the above four complexes. Key band assignments are given in Tables IV and V.

Conclusion

Raman spectra of $Os_2(O_2CCH_3)_4Cl_2$ taken at resonance with the axially polarized 383-nm band ($\pi(Cl) \rightarrow \pi^*(Os_2)$)[6] are characterized by long progressions in which the (axial) mode, ν_1, $\nu(OsOs)$ at 229 cm^{-1} acts as the progression-forming mode. This behavior, which is characteristic of A-term resonance Raman scattering of a_{1g} modes,[26] implies that the structural change consequent upon excitation to the resonant $\pi^*(Os_2)$ electronic state is substantial and principally along the Os–Os coordinate. The wavenumber of ν_1 is only slightly greater than that ($\sim$220 cm^{-1})[6] detected as structure to the long wavelength electronic bands of the complex, such as that ($\delta \rightarrow \delta^*$) at ca. 850 nm; clearly, the progression-forming mode in the electronic bands is likewise ν(OsOs), although the small ground-state to excited-state wavenumber change for ν_1 in these bands implies that, for such excited states, only very small changes occur to the osmium–osmium bond length.

Acknowledgment. We thank Johnson Mathey p.l.c. for the generous loan of platinum metal salts.

Registry No. $Os_2(O_2CCH_3)_4Cl_2$, 81519-41-7; $Os_2(O_2CCD_3)_4Cl_2$, 115603-76-4.

---

(25) Meester, P.; Fletcher, S. R.; Skapski, A. C. *J. Chem. Soc., Dalton Trans.* **1973**, 2575–2578.

(26) Clark, R. J. H.; Dines, T. J. *Angew. Chem., Int. Ed. Engl.* **1986**, *25*, 131–158.

A Symmetry-Based Procedure for the Determination of Molecular Geometry Changes Following Electronic Excitation. 1. Outline of the Qualitative Method

V. Bachler* and O. E. Polansky

Contribution from the Max-Planck-Institut für Strahlenchemie, Stiftstrasse 34-36, D-4330 Mülheim a.d. Ruhr, Federal Republic of Germany. *Received June 29, 1987*

Abstract: An extension of the Bader–Pearson concept to nondegenerate first excited states is presented which permits a qualitative determination of the relaxation pathway along which the molecular geometry changes following electronic excitation. A symmetry criterion for the relaxation pathway has been developed, according to which the most favored path is that which permits coupling of the first excited state with a large number of higher excited states close to the first excited state. Excited-state geometries of low symmetry are treated in a novel way by considering the pathway symmetry as a superposition of two different irreducible representations; numerical quantities are suggested for estimating the likelihood of particular representations to occur in the superposition. After determining the relevant symmetry species, the pathway is specified in greater detail by inspection of plots of the overlap function between interating orbitals, and a procedure for using such plots is described.

1. Introduction

Photochemical and spectroscopic properties of electronically excited molecules are frequently rationalized by referring to the form of the excited state potential energy surface. A photochemical reaction starts along that direction on the excited-state surface which leads to the smallest energy increase or even an energy minimum. Provided the pathway for an energy decrease is identical with a normal mode, a long vibrational progression in that mode may be observed in highly resolved electronic spectra.

Large scale configuration interaction methods proved to be reliable for the calculation of excited state potential energy surfaces.[1] The computational effort, however, would be diminished if a qualitative procedure were available predicting directions on the surface which are energetically favorable. Such a scheme would also be of use for the interpretation of large scale ab initio results, where a qualitative explanation of reliable results is often obscured by a maze of numbers. For ground-state surfaces the Bader–Pearson concept[2–4] relates explicitly the symmetry of the total wave function and the symmetry of reaction pathways. The essence of this concept is that the direction of a particular nuclear motion is energetically favorable if the electronic charge density can follow the motion easily. This simple concept led to a comprehensive rationalization of ground-state chemistry.[3] It has recently been incorporated by Bader into his theory of chemical reactivity which is based on a spatial partitioning of the electronic charge density.[5]

Few attempts have been made to apply the Bader–Pearson concept to electronically excited-state surfaces. A general rule for predicting the geometry of electronically excited molecules has been derived,[6] but for conjugated molecules it had to be extended.[7] Devaquet generalized the Bader–Pearson concept to first excited states[8] and applied it to a variety of electronically excited molecules.[8,9] However, in several instances it seemed difficult to discriminate between alternative directions for relaxation pathways. Nakajima analyzed carbon–carbon bond length changes of conjugated molecules following electronic excitation.[7] The bond length changes are correctly predicted, but molecular oribtals for σ-electrons are not explicitly considered. This restriction limits the procedure to nuclear motions in which planarity is retained. Bond length changes following electronic excitation can also be deduced from the ΔP-matrix as suggested by Zimmerman.[10] This matrix is defined as the difference be-

---

(1) For a review, see: Hirst, D. M. *Adv. Chem. Phys.* **1982**, *50*, 517. Bruna, P. J.; Peyerimhoff, S. D. *Adv. Chem. Phys.* **1987**, *67*, 1.

(2) Bader, R. F. W. *Can. J. Chem.* **1962**, *40*, 1164. Bader, R. F. W. *Mol. Phys.* **1960**, *3*, 137.

(3) Pearson, R. G. *Symmetry Rules for Chemical Reactions*; Wiley: New York, 1976.

(4) Pearson, R. G. *J. Mol. Struct., Theochem.* **1983**, *103*, 25.

(5) Bader, R. F. W.; MacDougall, P. J. *J. Am. Chem. Soc.* **1985**, *107*, 6788.

(6) Pearson, R. G. *Chem. Phys. Lett.* **1971**, *10*, 31.

(7) Nakajima, T.; Toyota, A.; Kataoka, M. *J. Am. Chem. Soc.* **1982**, *104*, 5610. Nakajima, T.; Toyota, A.; Fujii, S. *Bull. Chem. Soc. Jpn.* **1972**, *45*, 1022.

(8) Devaquet, A. *J. Am. Chem. Soc.* **1972**, *94*, 5626.

(9) Devaquet, A. *J. Am. Chem. Soc.* **1972**, *94*, 9012.

0002-7863/88/1510-5972$01.50/0 © 1988 American Chemical Society